Scaling of Gas-Centered Swirl-Coaxial Injectors

Malissa D.A. Lightfoot, Stephen A. Danczyk and Douglas G. Talley
Air Force Research Laboratory, Edwards AFB, CA

ABSTRACT

Robust design criteria and scaling for gas-centered swirl-coaxial (GCSC) injectors remain unclear despite much recent interest in using these injectors for LOX-hydrocarbon rocket engines. (The oxidizer is actually introduced as gas in the main-chamber injector.) A study of the behavior of the atomizing film in a GCSC injector has been undertaken as part of the development of improved design criteria. Using laser-sheet illumination the length of the film has been determined over a range of operating conditions and injector geometries. Experiments are performed using water and nitrogen as working fluids. Results show that the average film length relates to the momentum flux ratio and that the change in length per change in momentum flux ratio decreases at higher the momentum flux ratios. Such behavior is predicted from models of the injector.

INTRODUCTION

There has been much recent interest in moving from cryogenic hydrogen to hydrocarbons as the fuel for US rockets[1,2]. Hydrocarbon fuels require different injection techniques to produce high-performing, stable rocket engines. One approach to meet the different requirements of hydrocarbon-fueled systems has been the gas-centered swirl-coaxial (GCSC) injector. While this injector was used in Soviet rocket engines, it is relatively unstudied in the United States[1].

The lack of experience with GCSC injectors results in unclear design criteria. There are several requirements to consider when designing an injector for a rocket engine. The main requirement addressed in this work is the ability to generate a spray of good quality (reasonable droplet size and good spatial distribution of droplets). Further, since throttlability is often important in hydrocarbon-fueled rocket engines, a good quality spray must be achievable over a range of operating conditions. Throughout this work, the intact film length will be used as an indirect measure of atomization quality. Due to the atomization processes of GCSC injectors, a shorter film produces smaller, more uniformly distributed droplets than a long film[3]; more justification for this assertion is provided in the main text. The film length also provides additional design guidance by recommending the length of the injector outlet.

Gas-centered swirl-coaxial injectors are different from many injectors, especially those typically used in rocket engines, because atomization occurs within the injector body while the film is still bounded by a wall. Studies of atomization from wall-bounded films is generally confined to oceanic flows or annular flows in cooling tubes; both of these systems operate at mass flows rates which are substantially lower than those required in rocket engines[4]. As a result, it is difficult or impossible to leverage the predictive tools used in other systems to develop design criteria for rocket engines. This difficulty was recognized early in the US development of GCSC injectors[2] and models specific to GCSC injectors were sought. Further understanding determined that these injectors operate in a mode where stripping due to aerodynamic forces and turbulent structures are of primary importance[5]. This understanding enabled the development of a basic atomization model, based on stripping, which could be used as a basis for building a design methodology.

The main body of this paper focuses on experimental results in the context of this atomization model. Consequently, it opens with a very brief review of the model highlighting the key nondimensional parameter, momentum flux ratio, which should control the atomization of the spray. Contained in this review is an additional discussion of the importance of the intact film length. The experimental set-up is then detailed including key design parameters of GCSC injectors and their variation in this experiment. The main metric in these experiments is intact film length which is shown to predictably vary with design parameters and mass flow rates through the momentum flux ratio. The paper closes with a discussion of the implications of this finding on the design of GCSC injectors.

Report Documentation Page

Form Approved
OMB No. 0704-0188

1. REPORT DATE	2. REPORT TYPE	3. DATES COVERED
14 OCT 2008		

4. TITLE AND SUBTITLE	5a. CONTRACT NUMBER
Scaling of Gas-Centered Swirl-Coaxial Injectors (Preprint)	5b. GRANT NUMBER
	5c. PROGRAM ELEMENT NUMBER
6. AUTHOR(S)	5d. PROJECT NUMBER
	5e. TASK NUMBER
	5f. WORK UNIT NUMBER
7. PERFORMING ORGANIZATION NAME(S) AND ADDRESS(ES) **Air Force Research Laboratory (AFMC),AFRL/RZSA,10 E. Saturn Blvd.,Edwards AFB,CA,93524-7680**	8. PERFORMING ORGANIZATION REPORT NUMBER
9. SPONSORING/MONITORING AGENCY NAME(S) AND ADDRESS(ES)	10. SPONSOR/MONITOR'S ACRONYM(S)
	11. SPONSOR/MONITOR'S REPORT NUMBER(S)

12. DISTRIBUTION/AVAILABILITY STATEMENT
Approved for public release; distribution unlimited.

13. SUPPLEMENTARY NOTES

14. ABSTRACT

Robust design criteria and scaling for gas-centered swirl-coaxial (GCSC) injectors remain unclear despite much recent interest in using these injectors for LOX-hydrocarbon rocket engines. (The oxidizer is actually introduced as gas in the main-chamber injector.) A study of the behavior of the atomizing film in a GCSC injector has been undertaken as part of the development of improved design criteria. Using laser-sheet illumination the length of the film has been determined over a range of operating conditions and injector geometries. Experiments are performed using water and nitrogen as working fluids. Results show that the average film length relates to the momentum flux ratio and that the change in length per change in momentum flux ratio decreases at higher the momentum flux ratios. Such behavior is predicted from models of the injector.

15. SUBJECT TERMS

16. SECURITY CLASSIFICATION OF:			17. LIMITATION OF ABSTRACT	18. NUMBER OF PAGES	19a. NAME OF RESPONSIBLE PERSON
a. REPORT	b. ABSTRACT	c. THIS PAGE			
unclassified	**unclassified**	**unclassified**		**15**	

BACKGROUND

PREDICTIVE CAPABILITY AND VALUE OF FILM LENGTH

The typical operating conditions for GSCS injectors involve high gas velocities and high relative velocities between the gas and the liquid. As a result, the gas has a strong influence on the atomization behavior. Earlier investigations determined that stripping was likely the main mode by which droplets are produces and further postulated that the main driver which initiates the atomization process was the gas-phase turbulence[5]. From these findings, a formulation was developed which related the mass stripped from a single disturbance to various nondimensional parameters[5]. Five nondimensional parameters arose from this formulation—momentum flux ratio, Weber number of the liquid, Reynolds number of the liquid and parameters which are essentially Froude numbers. The pseudoFroude numbers indicate the importance of gravity and centripetal forces while the Weber and Reynolds numbers account for surface tension and viscous forces, respectively. The momentum flux ratio indicates the strength of lift and drag and of the friction forces related to the recirculation within the turbulent eddies. In a situation, as in typical operation of GCSC injectors, where aerodynamic forces dominate the momentum flux ratio is the key parameter in determining atomization behavior.

The idea that stripping is the main mode of atomization results in the relationship between spray quality and intact film length, particularly when the stripped disturbances are being generated by turbulence. Turbulence produces numerous discrete disturbances which are then stripped into single (or a very small number of) droplets. Due to the nature of turbulence, these disturbances are equally likely to occur throughout the surface of the film. This equal distribution means that atomization is distributed over the entire length of the film. As a result of the distributed nature of the atomization, there is no minimum film length prior to the onset of atomization. A minimum length might occur if, say, disturbances started to grow at the contact of the liquid and gas and needed a specific time to reach a size where they could be stripped; such behavior would be expected if disturbances were the result of hydrodynamic instabilities. As the contact time between the fluids increases, more mass is lost from the film. The rate of mass lost compared to that supplied sets the film length.

From this discussion it is clear that the film length is related to the amount of atomization occurring. Here the film length is also related to the droplet size and distribution. The earlier a droplet is produced the earlier it undergoes secondary droplet breakup producing even smaller droplets. At a given position on a film, a short film must produce more droplets than a longer film in order to achieve its short length; consequently, a short film produces more droplets earlier than a longer film. This difference results in smaller droplets in short films. (It is acknowledged that earlier-produced droplets are also more likely to collide possibly producing larger droplets, but the high gas velocity promotes breakup of any large droplets and also tends to produce droplet velocities hampering coalescence.) Additionally, earlier atomization promotes increased mixing between the gas and the droplets forming a solid spray with more evenly distributed droplets. If the film is intact to the injector exit then a sheet is formed which breaks up forming a hollow outer spray with a wide cone angle and large droplets. These droplets are much large due to the different atomization mechanism at work and because they are less likely to undergo secondary breakup due to the lower gas velocity far from the centerline.

Combining this information, it is expected that the film length should be strongly related to the momentum flux ratio. Furthermore, in these GCSC injectors the film length is a good qualitative indicator of spray quality: shorter film produce sprays with smaller droplets diameters and better droplet distribution. The remainder of this paper focuses on experimental results illustrating the link between film length (and, therefore, spray quality) and momentum flux ratio.

EXPERIMENTAL SET-UP

A basic schematic of a GCSC injector is given in Fig. 1. Liquid enters small inlet ports drilled tangential to the cylindrical outlet section. Unswirled gas enters through the center of the injector. In most GCSC atomizers a short section exists where the liquid is sheltered from the gas. This sheltered region allows the liquid flow to develop before coming in contact with the gas. The GCSC injector under study was modular allowing three parameters to be easily altered—the outlet radius, the initial film thickness (under the sheltered region) and the gas post radius at the end of the sheltering lip. Table 1 contains the list of injector geometries tested. The dimensions of the injectors are confirmed via a caliper

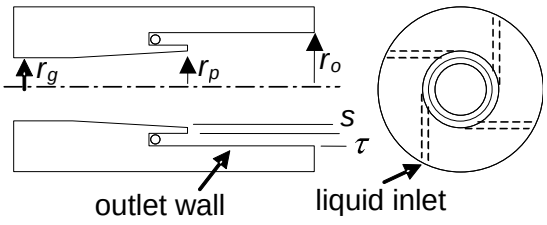

Figure 1: In this schematic of a gas-centered swirl-coaxial injector r_p represents the initial gas post radius, r_g the gas radius at the end of the sheltering lip, r_o the outlet radius, s the step height and τ the gap height. Table 1 lists the values of these dimensions used in the experiments.

Name	r_o (mm)	τ (mm)	r_g (mm)	s (mm)
ODHUTD	7.620	1.321	3.429	2.870
ODPDTD	7.620	1.321	5.461	0.838
ODHNTN	7.620	1.651	4.445	1.524
ODPDTN	7.620	1.651	5.461	0.508
ODHUTU	7.620	1.981	3.429	2.210
ODHDTU	7.620	1.981	5.461	0.178
ONPDTD	9.525	1.321	5.461	2.743
ONHNTD	9.525	1.321	6.350	1.854
ONPDTN	9.525	1.651	5.461	2.413
ONPNTN	9.525	1.651	6.350	1.524
ONPUTN	9.525	1.651	7.468	0.406
ONPNTU	9.525	1.981	6.350	1.194
OUHUTD	11.43	1.321	7.239	2.870
OUHDTD	11.43	1.321	9.271	0.838
OUPNTN	11.43	1.651	6.350	3.429
OUPUTN	11.43	1.651	8.407	1.372
OUHUTU	11.43	1.981	7.239	2.210
OUPUTU	11.43	1.981	8.407	1.041
OUHDTU	11.43	1.981	9.271	0.178

Table 1: The insert names and their attendant geometries are given above. The naming convention is to list the relative size of the (O)utlet and (P)ost radii and the film (T)hickness as either (D)own or (U)p from (N)ominal. In some inserts the (H)eight of the step plus film thickness is referenced instead of the gas post radius.

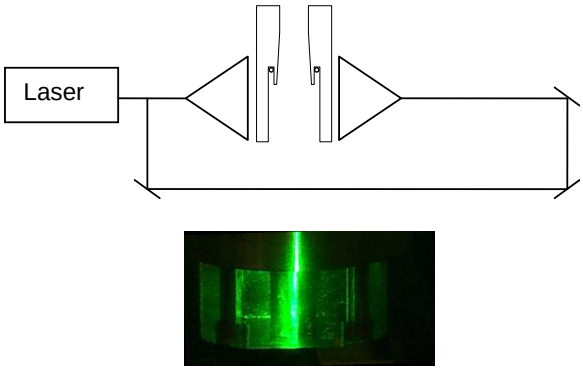

Figure 2: The laser set-up involved producing laser sheets (shown as triangles above) using cylindrical lenses. A photograph of the injector cup and laser sheet is also shown.

with an accuracy of +/-0.001 inch. Note that while changing the gas post radius changes the momentum flux ratio is also changes the height of the sheltering lip. This change obviously affects the gas flow, but it will be shown to effect on the film length only in terms of stability, not average length. The stability of the film length and its implications are addressed in greater detail in a separate paper[6].

The liquid in this experiment was water, and the gas was nitrogen. Flow rates were regulated by cavitating venturis and sonic nozzles, respectively, and upstream pressure regulation. The conversions from supply pressure to mass flow rate through the venturis and nozzles were calibrated via catch-and-weigh experiments. These conversions coupled with the accuracy of the pressure regulators produce an uncertainty of 0.227 g/s (0.0005 lb/s), ~0.25%, for the gas and liquid mass flow rates.

A dpss laser is split into two beams which are expanded to sheets to provide the illumination for high speed video. The sheets were introduced at the centerline of the injector 180° from one another; a schematic of this set-up is given as Fig. 2. Video was taken with a Vision Research Phantom v7.3 camera at 3000 and 6006 fps. The slower framing rate allowed a greater exposure time and more illumination and was taken to ensure the darkness of the 6006 fps video did not introduce a bias in the image processing. Because different operating conditions also effect the light available to the camera, it was important to establish that illumination did not impact measured film lengths. Comparison of results at several operating conditions and injector geometries showed no bias in average lengths between the two framing rates, so it was assumed that the image processing procedure was robust enough to handle any changes in lighting due to operating conditions. Consequently, only the results from the 6006 fps video are given here. The exposure time for the two framing rates were 310 μs and 110 μs.

Image processing was done via routines written in Matlab. Once the 14-bit image was converted to an array, vertical slices of the picture were examined. Each vertical slice was further divided into two areas where the film interface was likely to occur (since the film is visible in two locations due to the lighting used). These windows were based on the known edge of the injector body and the previous maximum location of the film (near the beginning, a maximum possible height based on the distance to the top of the sheltering lip was used). Within these windows the largest increase in intensity was marked as containing the film boundary and the largest increase over a single pixel within this area was chosen as the actual boundary. Lighting variations due to the turbulent nature of the flow and the atomization process occasionally produce difficulties, so care must be taken to ensure bright areas due to these variations are not mistaken labeled as film boundaries. This problem can be particularly troublesome if areas of the film near the wall appear bright. Despite filtering efforts and other improvement in image processing, only a percentage of the videos generated acceptable results. Acceptance of a video was based on user viewing; when the image processing is unsuccessful, it is generally very unsuccessful and poor results are easily identified. In many cases, one half of the image produced acceptable results while the other half did not; the good half of the video results are included here. The most common cause of failure in the image processing routine is insufficient or nonuniform lighting. Due to the lighting changes and the ever-thinning nature of the film, it is difficult to estimate the accuracy with which the length is actually captured. Additionally, the film length is not steady. The accuracy expected, then, could be based on the standard deviation of the measured film length which is reported later.

RESULTS

A time montage from a typical video is given as Fig. 3 and a single frame is given as Fig. 4. In the first frame of Fig. 3 and in Fig. 4, the outline of the injector geometry is overlaid as a reference. This overlay helps illustrate one of the complexities of the flow within the injector: the thickness of the liquid layer increases just downstream of the sheltered area. The gas flow over the sudden expansion of the lip creates a lower pressure, recirculating flow which the liquid fills to create a smoother transition. This change in flow patterns indicates that there are likely large changes in gas and liquid velocity throughout the injector outlet. For scaling purposes, however, a nondimensional parameter needs to be anchored to an easily calculable or measureable velocity. Discussion of the determination of the applicable velocities occurs later in this paper. Another observation from Fig. 3 is that the film length is not constant. While the range over which the film length varies is important—large variations can indicate unacceptable swings in spray quality or other undesirable unsteady behavior[6] --the main metric for scaling and spray quality is an average film length. Unsteady length behavior is addressed in this paper only from the standpoint of its impact on designing for an ideal injector length.

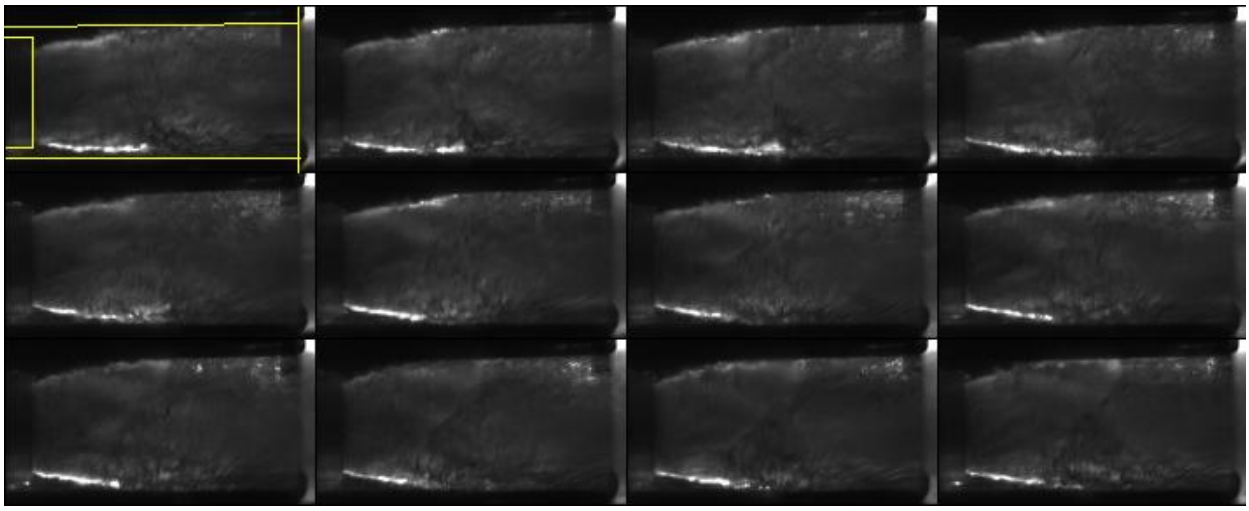

Figure 3: A typical film is shown here. The images are 0.33 ms apart and time runs left-to-right then top-to-bottom. Flow is from left to right. The outline on the first image shows the boundaries of the injector including the downstream edge of the lip initially separating the gas and liquid. (These frames show geometry ONPNTN operating at a momentum flux ratio of 338)

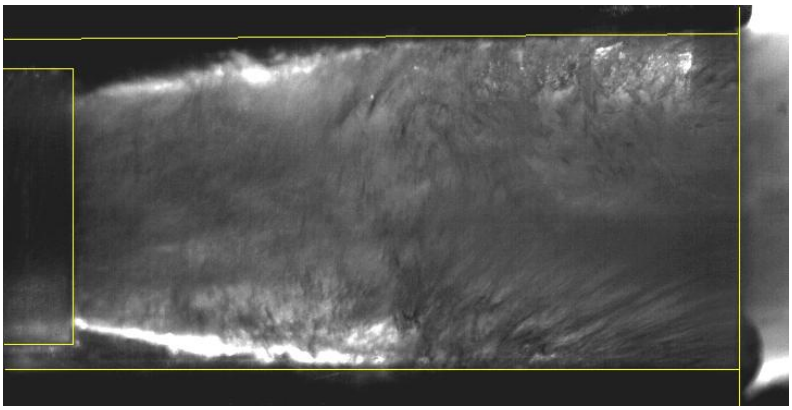

Figure 4: A typical image from the in-cup video is shown here. The edges of the injector body are highlighted including the sheltering lip. This image also shows the variation in lighting which can cause trouble in the image

The variation in film length also makes scaling somewhat more complex. The model should apply to the average length. Analysis indicated that a minimum of 4000 frames were needed to obtain statistically good average lengths. The lengths reported here are all determined from an average of 5000 consecutive images. Standard deviations of the film length are also given, along with test conditions, in Table 2 which appears at the end of this paper. The insert names refer back to those given in Table 1. Close examination of Table 2 shows that the complex flow in the injector can lead to differing lengths from the two "sides" of the injector under certain operating conditions. This difference is thought to relate to the swirling liquid flow. The differences lead to a scatter in the data and make scaling more difficult.

As discussed in the review at the outset of this paper, the energy of the gas flow drives the atomization in these injectors. Consequently, the film length (L) should decrease as the gas becomes more energetic (compared to the liquid). From the standpoint of the momentum flux ratio, the dependence of the film length on this ratio should be inverse—the film length decreases as the momentum flux ratio increases. This trend is, indeed, observed for all of the geometries tested and will be discussed in more detail below. First, some indication of the general character of the spray is given in relation to momentum flux ratio. At very low momentum flux ratios, a sheet is formed downstream of the exit. This regime is outside of that typically employed in rocket engines and will not be discussed here in any detail. At slightly higher momentum flux ratios two spray cones are created at the exit. The inner, solid cone contains small droplets created while the liquid was a film while the outer, "hollow" cone contains larger droplets (likely 0.25 mm or larger) created from ligaments which form after part of the film reaches the exit of the injector cup. The large outer droplets are obviously undesirable for combustion and the bimodal spatial distribution would be atypical and generally undesirable in combustion applications. As the momentum flux ratio increases, the number and size of the outer droplets decreases. Eventually, a single, solid cone spray is produced. While no measurement has yet been made of these droplets, they appear to have Sauter Mean Diameters (SMD) on the order of 10's of micrometers.

As discussed earlier, the velocity fields within the injector are complex, but a single velocity is needed for each phase when defining the momentum flux ratio. An inlet velocity could be used; however, the mass flow rates are the regulated quantities in the experiments and allow the calculation of a representative "mean" velocity within the injector based on injector geometry. The geometric parameters used to set the velocities require careful consideration and testing since the true velocity of import is that at the interface. It would be impractical or impossible to obtain this velocity experimentally. It might be possible to calculate this velocity using CFD, but these models remain impractically time-consuming and are unvalidated at the conditions considered here. Instead, a geometric parameter should be selected based on the injector parameters which are most likely to control the flow.

The liquid velocity vector is strongly controlled by the height under the sheltering step. The annular area sets an initial axial velocity of the liquid. The axial velocity is likely of more importance in this instance than the tangential or total velocity because it is the axial energy which competes with the gas phase during the atomization process. The gas is unswirled and initially contains no tangential component. The inlet velocity of the gas is controlled by the gas post diameter, but in many geometries

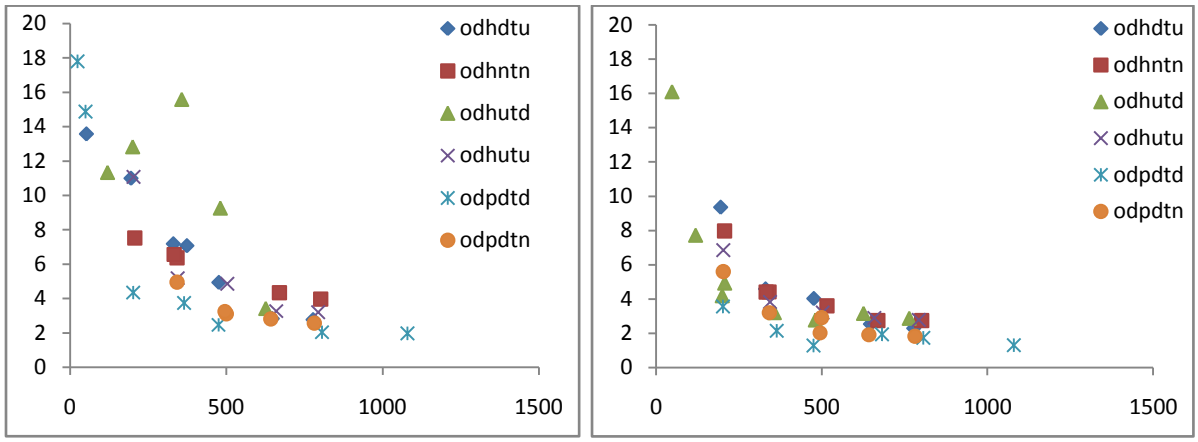

(a) (b)

Figure 5: Nondimensional length (film length divided by initial film thickness) is plotted as a function of momentum flux ratio based on initial film thickness and the gas-post radius added to the step height. Only the smallest outlet radius inserts are plotted here. The results from each side of the film are given as (a) and (b).

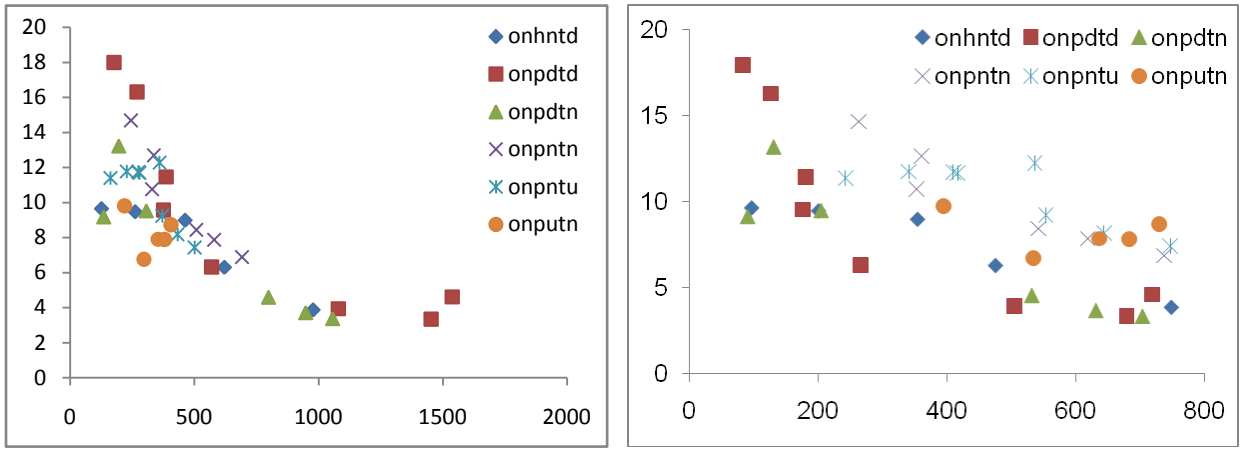

(a) (b)

Figure 6: Nondimensional length (film length divided by initial film thickness) is plotted as a function of momentum flux ratio based on initial film thickness and the gas-post radius added to the step height (b) or gas-post radius added to the initial film thickness (a). Only one side of the nominal outlet radius inserts is plotted here. Data from the other side of the injector yields similar results.

the post changes a short distance (a few diameters) upstream—becoming larger or smaller—altering the velocity. A further complication in the determination of the relevant geometry at which to determine the gas velocity is the likelihood that the gas flow is separated due to the geometric expansion despite the initial increase in liquid thickness. In support of this possible complication, the video shows areas of backflow in the cup, particularly at high momentum flux ratios. Several possibilities, then, exist to represent the gas flow—the mean velocity just prior to contact with the liquid (based on r_p^2), the mean velocity downstream after all the liquid is stripped (based on r_o^2) or some average along the film. The average along the film could be based on the velocity if the liquid did not fill-in along the step—$(r_o\text{-}s)^2$, the velocity based on the post plus initial film height (since the initial film height is also related to the length in various other ways, $(r_o\text{-}\tau)^2$) or the velocity based on the average between the post and outlet radius—$(r_o\text{-}(\tau+s)/2)^2$.

Clearly, other potential geometric parameters exist, but these were deemed to be the most likely, particularly the average of the post and outlet radius. All of these lead to slightly different definitions of

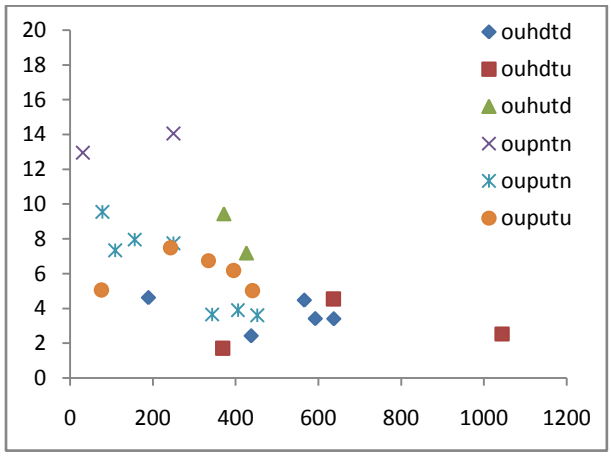

Figure 7: Nondimensional length (film length divided by initial film thickness) is plotted as a function of momentum flux ratio based on initial film thickness and the gas-post radius added to the step height. Only one side of the nominal outlet radius inserts is plotted here. There is very limited data from the other side of the injector.

the momentum flux ratio. All of these most-likely definitions were compared to the experimental data in an attempt to collapse the results from the various geometries onto a single curve. Using the velocity as if the film did not fill in the height of the step does a good job of collapsing the data for the smallest and largest outlet radii injectors, but does not do very well for the nominal outlet radius (Figs. 5 & 6). Conversely, using the velocity based on post height plus initial film height nicely collapses the nominal outlet radius results but does a poor job for the other radii (Fig. 7). The average of the two does the best overall job of collapsing the data across all three outlet geometries while within the individual outlet results the other scaling work slightly better. Figure 8 shows the most-outlying data (lowest and highest) for each outlet radius with the scaling based on average height. This scaling is recommended to apply to the largest range of geometry. Mathematically, then, momentum flux ratio is defined as $(\rho_\ell/\rho_g)(m_g/m_\ell)^2\{\tau(2r_o-\tau)/[r_o-(\tau+s)/2]^2\}^2$. As seen in Figs. 5-8 other definitions clearly show that the momentum flux ratio, in general, has a correspondence to the length. When different but somewhat sensible geometric parameters are chosen the data does not collapse to a single curve but falls into families of related curves. This collapse into families and not a single curve was expected—the complexity of the flow could, conceivably, resulted in the inability to produce a single scaling across the wide range of geometries and operating conditions considered and, indeed, scaling for subsets of geometries work better than scaling for the entire data set. Scaling subsets is substantially less powerful, however.

Note that as the momentum flux ratio increases its effect on the film length diminishes. So, a change in the momentum flux ratio from 200 to 300 nearly halves the film length while an change in the ratio from 650 to 750 produces only about a 20% reduction in the length. In some regards this is not surprising—there is a limit to how short the film can become. However, this may also be indicative of the specific geometry of this injector and the interplay between the separated gas flow and the atomizing film.

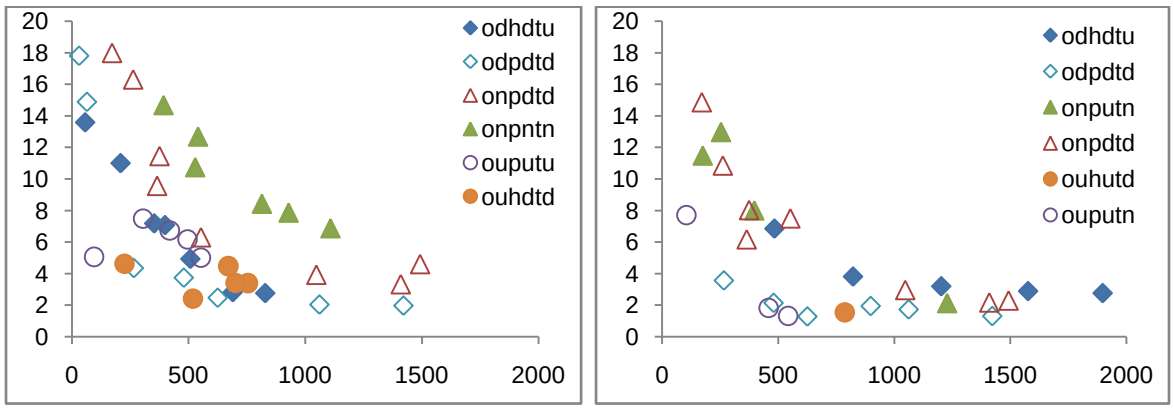

(a) (b)

Figure 8: Nondimensional length (film length divided by initial film thickness) is plotted as a function of momentum flux ratio based on initial film thickness and the average gas-post radius from contact with the film to exit. The most outlying geometries at each outlet radius are plotted. The results from each side of the film are given as (a) and (b).

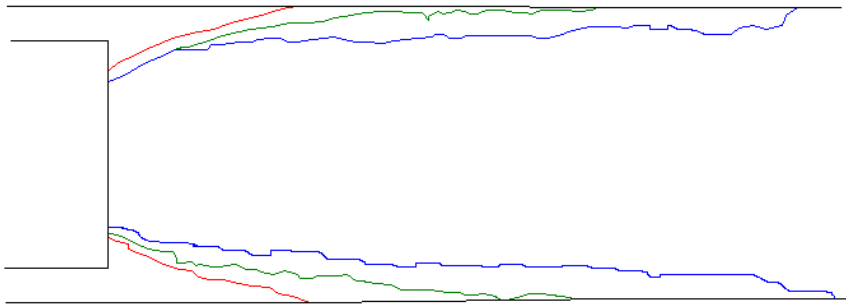

Figure 9: Representative profiles of a long, medium and short film. These profiles are from geometry ODHUTU at momentum flux ratios of 110, 484 and 823 respectively.

Figure 9 shows the different film profiles which occurs with long, medium and short films. As the film becomes very short, the expansion of the gas is more sudden and the more of the film is in contact with the slower moving recirculating gas flow (instead of the bulk gas flow). This should produce a fall-off in atomization rate or, equivalently, a fall-off in the change of film length with momentum flux ratio. This behavior has strong implications for injector design, particularly if the engine will need the ability to throttle. If geometries and operating conditions are chosen to maintain large momentum flux ratios, say above ~600, then the variation of average film length over the throttling range can likely be managed to within ~20%. Since the raw film lengths at these ratios are small, say near 5-10 mm, this is actually a modest change (1-2 mm). These experiments show that injectors can be designed to meet these momentum flux constraints and mixture ratio constraints. For example, geometry ONHNTD was tested at a momentum flux ratios of 767 and 1208 with corresponding mixture ratios of 2.2 and 2.7. The outlet radius in this geometry is at the high end of what would be expected in a rocket engine, but smaller injectors could still easily reach target mixture ratios between 2 and 3 with momentum flux ratios above 600.

Up to this point, scaling has been approached from the basis of the model which suggests momentum flux ratio is the important scaling parameter. Because this experiment was designed to help validate this approach, it is worthwhile to consider other possible scaling tactics. For example, there is a class of airblast atomizers similar to GCSC injectors except in the airblast atomizers the walls are much shorter and there is often an external (as well as internal) airflow. The atomization in these injectors typically occurs from a sheet. Some studies suggest that their atomization performance and intact sheet length scales with the air-to-fuel ratio, i.e. the ratio of mass flow rate of oxidizer to fuel[7]. This scaling has been used in other injector types as well[8]. Another utilized approach is to consider straight velocity ratios[9]. Finally, other nondimensional parameters appear in the model—Reynolds, Weber and pseudoFroude numbers. All of these possibilities were investigated and none of them collapsed the data across various geometries. As an example, Fig. 10 shows the nondimensional length as a function of mass flow ratio (mixture fraction) for selected geometries.

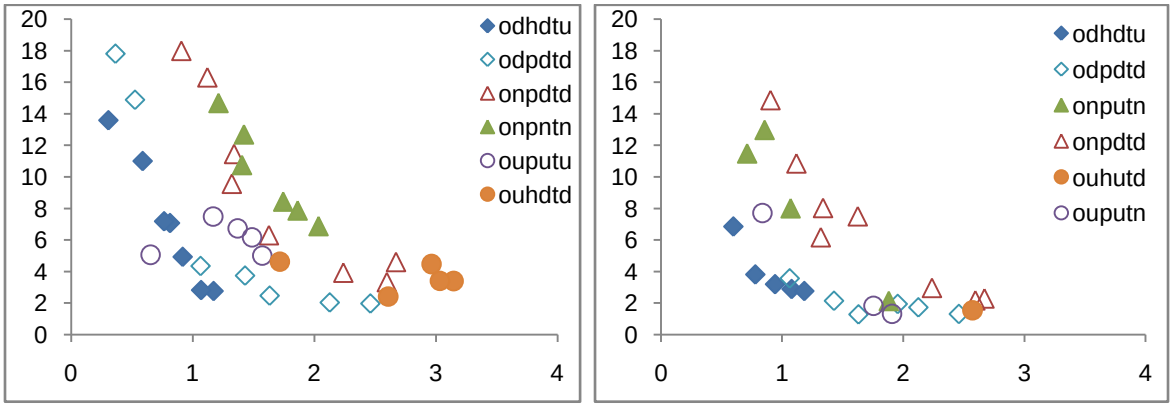

Figure 10: Nondimensional length (film length divided by initial film thickness) is plotted as a function of mixture ratio. The results from each side of the film are given as (a) and (b) and the same selection of geometries illustrated in Fig. 8.

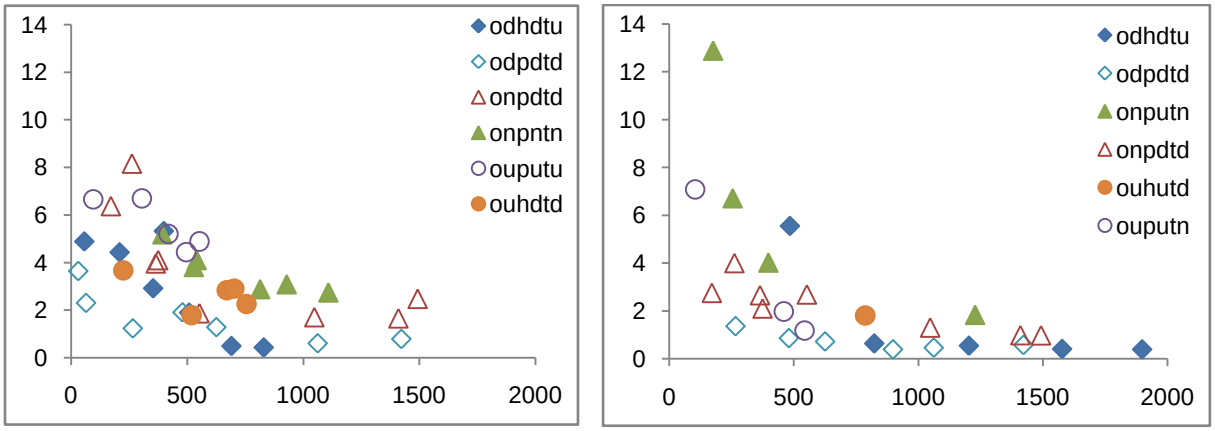

Figure 11: Standard deviation is plotted as a function of momentum flux ratio. The results from each side of the film are given as (a) and (b) and the same selection of geometries illustrated in Fig. 8.

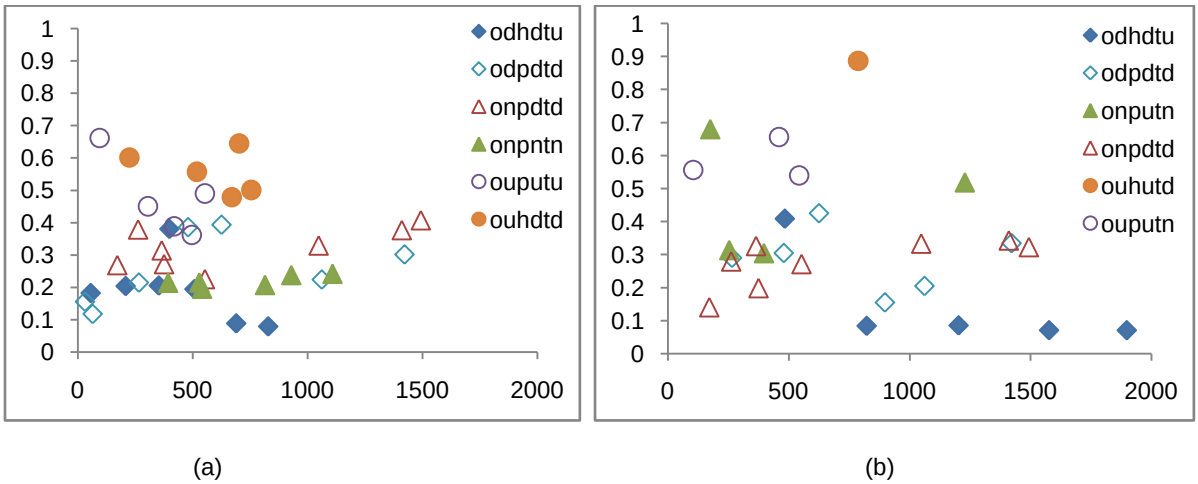

Figure 12: Nondimensionalized standard deviation (divided by film length) is plotted as a function of momentum flux ratio. The results from each side of the film are given as (a) and (b) and the same selection of geometries illustrated in Fig. 8.

One last finding of importance is the variation of film length in time. While, small changes in film length are unlikely to produce appreciable changes in the spray quality, they could cause problems for film lengths near the length of the injector. When the film becomes longer than the injector, even locally, some number of very large, undesirable droplets are produced. In designing an injector, particularly for a throttling engine, the designer must be cognizant of the variation in length to maintain good spray quality. On the other hand, there are stiff penalties for designing an injector which is too long. In addition to needless increasing the engine weight, injectors which are too long may have flames anchored in their cups[1]. While an anchored flame is good, this anchoring location would lead to appreciable heating of the injector faceplate and could cause melting. Length variations in time, indicated by standard deviations of the length data, are reported in Fig. 11. The results at the low momentum flux ratios may be artificially reduced because film lengths cannot be measured in excess of the injector length, so any variation above that length is not captured in this data. In general, however, it can be noted that the standard deviation decreases as the momentum flux ratio increases, possibly leveling off at momentum flux ratios above ~600. As with the earlier length findings, this result suggests that the optimum operation conditions are at high momentum flux ratios. As aforementioned, the length also decreases with momentum flux ratio, so

the raw deviation is not the complete story. Figure 12 reports the variation in standard deviation normalized by the average film length as a function of momentum flux ratio. Here it is seen that the relative variation with is length nearly constant value. Given the difficulties in accurately reporting the standard deviations of long films at lower momentum flux ratios, it is conceivable that the variation in film length as a function of average film length is essentially constant regardless of momentum flux ratio. Again, then, to minimize the temporal variation in length the film should be as short as possible and high momentum flux ratios should generate the best performance.

CONCLUSIONS

A gas-centered swirl-coaxial injector has been examined with a range of geometries and operating conditions. The geometry of the gas inlet and liquid inlet as well as the geometry of the lip separating the two phases has been varied. A range of mass flow rates of the two phases has also been examined. The main objective of this testing was to find a parameter which allowed the prediction of atomization performance. Here, atomization performance is linked to the length of the intact film inside the injector. A model is briefly reviewed which suggests this length is related to the momentum flux ratio between the gas and liquid.

The experimental results presented here do, indeed, illustrate that the average film length (and, at least qualitatively, spray quality) can be predicted based on the momentum flux ratio. The momentum flux ratio is defined using the initial film thickness and the average gas-post radius from liquid contact to the exit--$\left(\rho_\ell/\rho_g\right)\left(m_g/m_\ell\right)^2\{\tau(2r_o-\tau)/[r_o-(\tau+s)/2]^2\}^2$. Furthermore, the average film length may be controlled over a range of throttle conditions because its dependence trails off as the momentum flux ratio increases. For example, with the ODPDTD geometry a momentum flux ratio range of 625 to 1062 (with attendant mixture ratio range of 1.6-2.1) produces a change in average length of from 3.25 to 2.69 mm, about a 20% change. Also of importance, the transient change in film length also trails as momentum flux ratio increases. This dependence is important so that the injector can be correctly sized to prevent melting of the faceplate (too long) and poor atomization quality (too short). These recommendations are based on a wide array of geometric and operating conditions and built on the foundation of a model which recommended the momentum flux ratio as the key scaling parameter.

ACKNOWLEDGEMENTS

The assistance of Mr. Albert Wu was instrumental in developing the image processing routines used herein. The help of Captain Kristen Clark in completing these experiments is also greatly appreciated.

REFERENCES

[1]Cohn, R.K., et al., *Swirl Coaxial Injector Development*. 2003: Reno, NV.

[2]Strakey, P., R.K. Cohn, and D.G. Talley, *The Development of a Methodology to Scale Between Cold-Flow and Hot-Fire Evaluations of Gas-Centered Swirl Coaxial Injectors*, in *52nd JANNAF Propulsion Meeting*. 2004: Las Vegas, NV.

[3]Lightfoot, M.D.A., S.A. Danczyk, and D. Talley, *Atomization Rate of Gas-Centered Swirl-Coaxial Injectors*, in *ILASS Americas 21st Annual Conference on Liquid Atomization and Spray Systems*. 2008: Orlando, FL.

[4]Lightfoot, M.D.A., *A Fundamental Classification of Atomization Processes.* Submitted to Atomization and Sprays, 2008.

[5]Lightfoot, M.D.A., S.A. Danczyk, and D. Talley, *Atomization Performance Predictions of Gas-Centered Swirl-Coaxial Injectors*, in *54th JANNAF Propulsion/5th MSS/3rd LPS/2nd SPS Joint Technical Meeting*. 2007.

[6]Lightfoot, M.D.A., S.A. Danczyk, and D. Talley, *Scaling of Gas-Centered Swirl-Coaxial Injectors*, in *JANNAF 6th Modeling and Simulation/4th Liquid Propulsion/3rd Spacecraft Propulsion Joint Subcommittee Meeting*. 2008: Orlando, FL.

[7]Carvalho, I.S. and M.V. Heitor, *Liquid Film Break-up in a Mode of a Prefilming Airblast Nozzle.* Experiments in Fluids, 1998. **24**(5-6): p. 408-415.

[8]Lee, S.G., et al., *Turbulent Disintegration Characteristics in Twin Fluid Counterswirling Atomizer*. 2001: Reno, NV.

[9]Lasheras, J.C. and E.J. Hopfinger, *Liquid jet instability and atomization in a coaxial gas stream.* Annual Review of Fluid Mechanics, 2000. **32**: p. 275-290.

Table 2: The operating conditions are given for the tests discussed here and reported in the figures.

Geometry	Gas mass flow	Liquid mass flow	Mom flux ratio	Film Length	Film Length	Stand Dev	Stand Dev
	kg/s	kg/s		mm (side a)	mm (side b)	mm (side a)	mm (side b)
odhdtu	0.0229	0.0282	399	14		5.3	
odhdtu	0.0242	0.0794	56	26.9		4.9	
odhdtu	0.0339	0.0578	208	21.8	18.5	4.4	5.2
odhdtu	0.0446	0.0487	508	9.8	8	1.9	1.3
odhdtu	0.0449	0.0588	352	14.2	9.1	2.9	1.5
odhdtu	0.0679	0.058	829	5.5	4.5	0.4	0.4
odhdtu	0.0681	0.0638	690	5.6	5	0.5	0.5
odhntn	0.0344	0.0435	406	12.4	13.2	10.1	2.7
odhntn	0.0453	0.0445	671	10.5	7.3	2.4	1.1
odhntn	0.0456	0.0365	1014		6		1.1
odhntn	0.0461	0.0459	653	10.9	7.3	2.6	1
odhntn	0.0685	0.0439	1576	6.5	4.5	1.3	0.4
odhntn	0.0686	0.0482	1316	7.2	4.5	1.6	0.4
odhutd	0.0222	0.0424	137		21.3		9.7
odhutd	0.023	0.028	337	15	10.2	14.1	1.9
odhutd	0.0351	0.0325	584		6.5		1
odhutd	0.0457	0.0278	1353	12.2	3.7	11	0.7
odhutd	0.046	0.0325	1005	20.6	4.2	11.6	0.7
odhutd	0.0673	0.0325	2149		3.8		0.5
odhutd	0.0674	0.036	1761	4.5	4.2	0.7	0.4
odhutd	0.068	0.0642	563	17	5.5	7.7	0.4
odhutu	0.0343	0.0575	484	22	13.6	11.7	5.6
odhutu	0.0452	0.0581	823	10.3	7.6	1.2	0.6
odhutu	0.0457	0.0486	1203	9.6	6.3	2.5	0.5
odhutu	0.0683	0.0634	1577	6.5	5.7	0.4	0.4
odhutu	0.0684	0.0578	1898	6.3	5.5	0.5	0.4
odpdtd	0.0228	0.0435	65	19.7		2.3	
odpdtd	0.0233	0.0641	31	23.5		3.6	
odpdtd	0.0336	0.0316	266	5.7	4.7	1.2	1.4
odpdtd	0.0456	0.028	625	3.3	1.7	1.3	0.7
odpdtd	0.0458	0.0321	480	4.9	2.8	1.9	0.9
odpdtd	0.0682	0.0277	1422	2.6	1.7	0.8	0.6
odpdtd	0.0684	0.0322	1062	2.7	2.3	0.6	0.5
odpdtd	0.0687	0.0352	898		2.6		0.4
odpdtn	0.0342	0.0437	241		9.3		2.4
odpdtn	0.0452	0.0368	594	5.2	4.8	0.9	1
odpdtn	0.0452	0.0444	407	8.2	5.3	1.5	0.8
odpdtn	0.0674	0.0438	929	4.3	3	0.3	0.3
odpdtn	0.0676	0.0485	764	4.7	3.2	0.4	0.4
odpdtn	0.0678	0.0554	589	5.4	3.3	0.6	0.4
onhntd	0.045	0.0459	157	12.7	14.6	6.9	8.1
onhntd	0.0452	0.032	324	12.5		6.7	
onhntd	0.0575	0.0265	767	8.3		4.7	
onhntd	0.0582	0.031	572	11.9		6.4	
onhntd	0.0679	0.0249	1208	5.1		3.3	
onpdtd	0.0392	0.0434	171	23.8	19.6	6.4	2.8
onpdtd	0.0399	0.0303	365	12.6	8.2	4	2.7
onpdtd	0.056	0.0501	262	21.5	14.3	8.2	4
onpdtd	0.0581	0.0434	375	15.1	10.6	4.1	2.1
onpdtd	0.059	0.0264	1048	5.2	3.9	1.7	1.3
onpdtd	0.0592	0.0364	553	8.3	9.9	1.9	2.7
onpdtd	0.0638	0.0246	1410	4.4	2.9	1.7	1
onpdtd	0.0685	0.0257	1493	6.1	3	2.5	1

Geometry	Gas mass flow	Liquid mass flow	Mom flux ratio	Film Length	Film Length	Stand Dev	Stand Dev
	kg/s	kg/s		mm (side a)	mm (side b)	mm (side a)	mm (side b)
onpdtn	0.0386	0.0542	176	15.2	19	14.2	12.9
onpdtn	0.0561	0.0656	254	21.8	21.4	8	6.7
onpdtn	0.0568	0.0329	1034	7.6		2.5	
onpdtn	0.058	0.0542	398	15.7	13.2	3.8	4
onpdtn	0.0624	0.0332	1228	6.1	3.5	2.8	1.8
onpdtn	0.0659	0.0332	1369	5.6		2.9	
onpntn	0.0457	0.0326	529	17.7	7.3	3.8	4.1
onpntn	0.0541	0.0447	393	24.2		5.2	
onpntn	0.0566	0.0325	814	13.9		2.9	
onpntn	0.0609	0.0327	929	13		3.1	
onpntn	0.0667	0.0328	1108	11.4		2.7	
onpntn	0.0672	0.0474	541	21		4.1	
onpntu	0.052	0.0574	335		15.1		7.4
onpntu	0.0520	0.0574	336	22.6	17.6	8.2	9.7
onpntu	0.0535	0.0396	746	24.3		2.8	
onpntu	0.0545	0.0397	769	18.3	20.2	4.2	3.7
onpntu	0.0590	0.0398	896	16.2		3	
onpntu	0.0601	0.0559	473	23.3		4.7	
onpntu	0.0624	0.0394	1024		12.4		3.7
onpntu	0.0629	0.0394	1039	14.7	16.6	2.8	3.1
onpntu	0.0652	0.0547	578	23.2		4.9	
onpntu	0.0655	0.0555	569	23.3	17.3	7.4	4.7
onpntu	0.0546	0.0573	371	23.2	19.2	4.9	4.8
onpntu	0.0652	0.0532	614	23.3	15.6	7.4	6.4
onputn	0.0561	0.0324	593	11.2	6.1	2.5	4.4
onputn	0.0614	0.0325	707	13	6.5	2.8	3.8
onputn	0.0637	0.0326	758	13		3	
onputn	0.066	0.0326	810	14.4	5.9	3.6	2.9
onputn	0.0695	0.0467	438	16.2		4	
ouhdtd	0.0457	0.0266	225	6.1		3.7	
ouhutd	0.0672	0.0261	787		2		1.8
ouhdtd	0.068	0.0261	519	3.2		1.8	
ouhdtd	0.0786	0.0265	671	5.9		2.8	
ouhdtd	0.0788	0.0251	755	4.5		2.3	
ouhdtd	0.0789	0.026	702	4.5		2.9	
ouhdtu	0.046	0.032	383	3.4		2.6	
ouhdtu	0.068	0.036	661	9		3.9	
ouhdtu	0.0689	0.0285	1084	5		2.9	
ouhutd	0.0672	0.0261	787	9.5		4.8	
ouhutd	0.0672	0.028	686	12.5		7.5	
oupntn	0.0336	0.0635	68	21.4		9.6	
oupntn	0.0679	0.0454	540	23.2		9.3	
ouputn	0.0449	0.0454	146	12.1		3.2	
ouputn	0.045	0.0236	543	6.4	2.2	2.7	1.2
ouputn	0.053	0.0263	606	5.9		2.8	
ouputn	0.0531	0.0635	104	15.8	12.7	9.9	7.1
ouputn	0.0533	0.0304	459	6	3	3.8	2
ouputn	0.0537	0.0454	209	13.1		5.2	
ouputn	0.0679	0.0454	334	12.8		7.2	
ouputu	0.0488	0.0748	95	10		6.6	
ouputu	0.0529	0.0454	305	14.8		6.7	
ouputu	0.054	0.0363	496	12.3		4.4	
ouputu	0.057	0.0363	553	10		4.9	
ouputu	0.0621	0.0454	419	13.4		5.2	